European Journal of Pharmaceutics and Biopharmaceutics 134 (2019) 60–67

Contents lists available at ScienceDirect

European Journal of Pharmaceutics and Biopharmaceutics

journal homepage: www.elsevier.com/locate/ejpb

Research paper

Cubosomes for topical delivery of the antimicrobial peptide LL-37

Lukas Boge[a,b,*], Karin Hallstensson[a], Lovisa Ringstad[a], Jenny Johansson[a], Therese Andersson[a], Mina Davoudi[c], Per Tomas Larsson[d], Margit Mahlapuu[e,f], Joakim Håkansson[a], Martin Andersson[b]

[a] RISE Research Institutes of Sweden, Box 857 SE-50115, Borås, Sweden
[b] Department of Chemistry and Chemical Engineering, Applied Chemistry, Chalmers University of Technology, Göteborg, Sweden
[c] Division of Dermatology and Venereology, Department of Clinical Sciences, Lund University, Sweden
[d] RISE Innventia AB, Stockholm, Sweden
[e] Promore Pharma AB, Karolinska Institutet Science Park, Solna, Sweden
[f] The Lundberg Laboratory for Diabetes Research, Department of Molecular and Clinical Medicine, The Sahlgrenska Academy at University of Gothenburg, Gothenburg, Sweden

ARTICLE INFO

Keywords:
Cubosome
LL-37
Antimicrobial peptide
Topical delivery
Infection
Skin irritation
Proteolysis

ABSTRACT

In this study, the use of cubosomes for topical delivery of the antimicrobial peptide (AMP) LL-37 was investigated. Topical delivery of AMPs is of great interest for treatment of skin infections caused by bacteria, such as *Staphylococcus aureus*. AMP containing cubosomes were produced by three different preparation protocols and compared: (i) pre-loading, where LL-37 was incorporated into a liquid crystalline gel, which thereafter was dispersed into nanoparticles, (ii) post-loading, where LL-37 was let to adsorb onto pre-formed cubosomes, and (iii) hydrotrope-loading, where LL-37 was incorporated during the spontaneously formed cubosomes in an ethanol/glycerol monooleate mixture. Particle size and size distribution were analyzed using dynamic light scattering (DLS), liquid crystalline structure by small angle x-ray scattering (SAXS) and release of LL-37 by a fluorescamine assay. Proteolytic protection of LL-37 as well as bactericidal effect after enzyme exposure was investigated. The skin irritation potential of cubosomes was examined by an *in vitro* epidermis model. Finally, the bacterial killing property of the cubosomes was examined by an *ex vivo* pig skin wound infection model with *Staphylococcus aureus*. Data showed that a high loading of LL-37 induced formation of vesicles in case of cubosomes prepared by sonication (pre-loading). No release of LL-37 was observed from the cubosomes, indicating strong association of the peptide to the particles. Proteolysis studies showed that LL-37 was fully protected against enzymatic attacks while associated with the cubosomes, also denoting strong association of the peptide to the particles. As a consequence, bactericidal effect after enzyme exposure remained, compared to pure LL-37 which was subjected to proteolysis. No skin irritation potential of the cubosomes was found, thus enabling for topical administration. The *ex vivo* wound infection model showed that LL-37 in pre-loaded cubosomes killed bacteria most efficient.

1. Introduction

Antimicrobial resistance is today listed as one of the biggest challenges in the global health sector [1]. Until today, infections have effectively been treated with various types of antibiotics, such as penicillin. A post antibiotic era is not far from becoming the reality in the 21st century, as more and more bacteria are developing high level resistance to many available antibiotics [2]. Due to the fast development of multi resistant bacteria, even less severe infections may be difficult to treat in a near future. Colonization of these bacteria in wounds is a serious threat. For example, treatment of surgical site infections (SSIs), skin and soft tissue infections (SSTIs) and burn wound infections all rely on efficient antibiotic therapies. The most common bacteria causing these infections are *Staphylococcus aureus* and its methicillin resistant analogue, *Pseudomonas aeruginosa* and multi-drug resistant variants, *Staphylococcus epidermis* and *Escherichia coli* [3–8]. An alternative to conventional antibiotics that could be one type of future treatments are antimicrobial peptides (AMPs) [9]. They provide a combination of advantages displaying fast and unspecific broad-spectrum bactericidal properties as well as being less prone to develop antimicrobial resistance bacteria [9–11]. However, the low specificity of AMPs, has been suggested to limit their therapeutic use to topical delivery, because of hemolytic and toxicity activity at high concentrations [10]. Moreover, most AMPs are susceptible to chemical and proteolytic

* Corresponding author.
E-mail address: lukas.boge@ri.se (L. Boge).

https://doi.org/10.1016/j.ejpb.2018.11.009
Received 23 September 2018; Received in revised form 7 November 2018; Accepted 12 November 2018
Available online 13 November 2018
0939-6411/

degradation at physiological conditions and need a protective matrix in order to enable efficient treatments [12–14]. Liquid crystalline nanoparticles (LCNPs), e.g. cubosomes, offer a unique possibility of encapsulating and protecting protein and peptide drugs from degradation [15–17]. Cubosomes consists of folded lipid bilayers curved in three-dimensional space with interwoven water channels. The complex amphipathic structure of the cubosome makes incorporation of hydrophilic (in the aqueous channels), hydrophobic (in the lipid bilayers) and amphiphilic drugs (at the bilayer-water interface) possible [18]. Several AMPs have successfully been incorporated in cubosomes such as the plectasin derivative AP114 [19–21], the human kininogen derivative DPK-060 [19,20], gramicidin A, melittin, and alamethicin [22] as well as the human cathelicidin LL-37 [23,24]. LL-37 is found in different cells, tissues and body fluids [25]. LL-37 is a 37 amino acid long amphiphilic and water soluble peptide (molecular weight 4491 Da) having a net charge of +6.3 at pH 5.5. In addition to its broad spectrum bacterial killing and immunomodulatory properties, LL-37 also promotes healing of chronic wounds [25–27] and is an important part of the innate immune system of the skin. Thus, LL-37 is an interesting candidate for topical treatment of bacterial infections. The peptide mainly exhibits a random coil conformation in aqueous solution, but changes its secondary structure to α-helical upon membrane interaction [28,29]. It is suggested that LL-37 uses a toroidal pore/carpet-like mechanism of action [30]. The exact mechanism of action is debated and is also suggested to depend on the concentration [28]. However, LL-37 is sensitive to proteolytic degradation, which has limited its therapeutical use [26]. Notably, adsorption of LL-37 onto glycerol monooleate (GMO) cubosomes has shown to protect the peptide from degradation by elastases that can be present at a bacterial infection site [20]. Lipid based colloidal systems have shown ability to effectively deliver and transport drugs to and through the skin as they can help fluidizing skin lipids [31–33]. Furthermore, LCNPs can enhance the skin penetration and delivery of several active substances, such as peptides, vitamins, herbal extracts, vaccine adjuvants and anti-inflammatory drugs with no observed skin irritation [34–38]. Moreover, cubosomes were recently used to deliver photosensitizers for photodynamic therapy (PDT) of human skin melanoma cells [39].

In this work, we have explored the use of GMO-based cubosomes for topical delivery of LL-37. GMO is non-toxic and biodegradable lipid, listed as an “inactive ingredient” approved in topical (and oral) drug products by the U.S. Food and Drug Administration (FDA) and was therefore chosen for preparation of the cubosomes [40,41]. Three different peptide loading strategies were used and compared, to reveal any differences in the properties of the cubosomes: (i) pre-loading, where LL-37 was incorporated into the liquid crystalline gel, which thereafter was dispersed into nanoparticles, (ii) post-loading, where LL-37 was allowed to adsorb onto pre-formed cubosomes, and (iii) hydrotrope-loading, where LL-37 was incorporated during the spontaneously formed cubosomes from an ethanol/glycerol monooleate mixture. Pre-loaded cubosomes have the advantage that the incorporated AMP is likely to take part of the LC structure, enabling high peptide encapsulation efficacy [19]. Post-loaded particles are subjected to a heat-treatment cycle before loading of the peptide, resulting in a sterile cubosome dispersion, usually displaying a reduced fraction of vesicles that are often present in cubosomes prepared by sonication [42]. The hydrotrope preparation method has the advantage that no high shear mixing equipment is needed, reducing the manufacturing cost [43,44].

The size and size distribution of the cubosomes were characterized by dynamic light scattering (DLS), their structure was analyzed by small-angle x-ray scattering (SAXS) and release of LL-37 was monitored by dialysis in combination with a fluorescamine assay. The proteolytic protection of LL-37 in the cubosomes was studied after incubation with enzymes that may be present in infected wounds and the antibacterial effect after proteolysis was assessed by radial diffusion assay (RDA). The skin irritation potential of the cubosomes was tested using an *in vitro* epidermis model and the bactericidal effect was investigated with an *ex vivo* pig skin wound infection model.

2. Materials and methods

2.1. Materials

Glycerol monoleate Capmul-90 EP/NF was obtained as a gift from Abitec Corp. (Columbus, USA) with composition 93.3% and 6.3% mono and di-glycerides, respectively, and C18:1 (oleyl content) > 95%. The triblock co-polymeric stabilizer Poloxamer 407 (Kolliphor P407, approx. 12.500 g/mol) was purchased from BASF (Ludwigshafen, Germany) and antimicrobial peptide LL-37 (LLGDFFRKSKEKIGKEFKRIVQRIKDFLRNLVPRTES), peptide content 81.8% (purity 94.7%), was synthesized and provided by PolyPeptide Laboratories (Limhamn, Sweden). Buffer solutions were always sterile filtered prior use.

2.2. Cubosome preparation

Pre-loaded: Liquid crystalline (LC) gels were prepared and dispersed into cubosomes as described previously [19]. Briefly, molten GMO (45 °C) was mixed with a water solution containing LL-37 to reach a concentration of 0, 1, 3 or 6 w% peptide in the LC gels, at a mass ratio of GMO:water of 70:30. Dispersions were made by fragmenting 0.5 g LC gel in 9.5 g 0.5% Poloxamer 407 (dissolved in 20 mM sodium acetate buffer pH 5.5) using a Ultra-Turrax high shear mixer followed by tip-sonication, resulting in LL-37 concentration of 0, 0.5, 1.5 or 3 mg/mL.

Post-loaded: 1.0 g of cubic LC gel (not containing LL-37) was prepared and dispersed as for pre-loaded particles in 9.0 g MilliQ-water containing 1% P407 stabilizer. A heat-treatment cycle of the sample was thereafter performed in order to reduce the number of vesicles [42] in a Laboklav 25 autoclave (SHP Steriltechnik AG, Schloss Detzel/Satuelle, Germany) at 121 °C for 20 min. The total autoclave cycle was ca. 75 min, including time required to heat-up and cooling down to room temperature. The cubosome dispersion was thereafter diluted 1:1 with 40 mM sodium acetate buffer pH 5.5 followed by addition of LL-37 as a small aliquot. Samples were prepared with LL-37 concentration of 0, 0.5, 1.5 or 3 mg/mL.

Hydrotrope: Cubosomes were also produced by the hydrotrope method [44]. Briefly, 0.35 g molten GMO (45 °C) was mixed with 0.35 mL ethanol (99.5%) to form an isotropic solution. 300 μL of LL-37 dissolved in 20 mM acetic acid buffer (pH 5.5) was added dropwise under magnetic stirring (ca 1000 rpm), followed by slow addition of 8.7*g* 0.5% Poloxamer 407 dissolved in buffer. Samples were prepared with LL-37 concentration of 0, 0.5, 1.5 and 3 mg/mL.

2.3. Dynamic light scattering (DLS)

Particle size and its distribution were determined by dynamic light scattering (DLS) using a Zetasizer Zen3600 (Malvern Instruments Ltd., Worcestershire, U.K.) at 20X dilution of the samples in MilliQ-water. The hydrodynamic radius, assuming spherical particles, was calculated by the software using Stoke-Einsteiń relation to describe the Brownian motion of the particles. Each sample was measured in triplicate using disposable plastic cuvettes at 25 °C.

2.4. Small angle x-ray scattering (SAXS)

Characterization of the LC structures was performed using small angle x-ray scattering (SAXS) with a SAXSpoint 2.0 instrument (Anton Paar, Graz, Austria) equipped with a Microsource x-ray source (Cu Kα radiation, $\lambda = 1.5418$ Å) and a Dectris 2D CMOS Eiger R 1 M detector. Gels were placed in a steel sample holder between two kapton windows, resulting in a sample thickness of approximately 1 mm. Liquid samples were placed in quartz capillaries (D = 1.5 mm, wall thickness 0.01 mm, Hilgenberg GmbH, Germany) and sealed with epoxy glue. The exposure per sample was 10 min for gel samples and 20–120 min

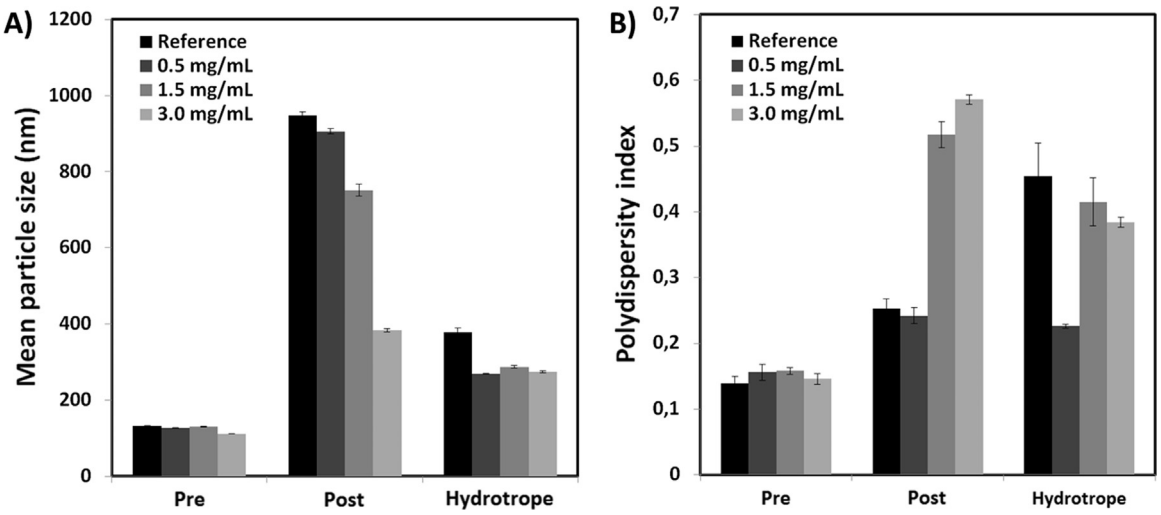

Fig. 1. Particle size (A) and polydispersity index (B) of the LCNP with 0 (reference) and 0.5, 1.5 and 3.0 mg/mL LL-37 prepared by pre-loading of LL-37 (Pre), post-loading of LL-37 (Post) and by the hydrotrope method (Hydrotrope). Data is presented as mean ± standard deviation (N = 3). The PDI of LCNPs prepared by the hydrotrope method at 0.5 mg/mL LL-37 is lower compared to the other PDI's due to absence of small fraction of larger particles, present in the other Hydrotrope samples, that has a great influence on PDI.

for liquid samples at a sample to detector distance of 576 mm. Identifications of the LC phases were done according to Bragg peak spacings [45].

2.5. Release of antimicrobial peptide

Release of AMP was monitored trough dialysis and fluorescamine assay as described elsewhere [20,21]. Briefly, 1 mL of the sample was placed in a dialysis device (Float-A-Lyzer® G2 100 kDa MWCO, Spectrum Laboratories Inc., Rancho Dominques, USA) allowed to dialyze in 20 mL, 20 mM sodium acetate buffer pH 5.5 at 22 ± 1 °C. 200 µL samples were withdrawn after 0, 1, 2, 4, 6 and 24 h of dialysis. Peptide quantification was performed with a fluorescamine assay, using a plate reader (CLARIOstar® GMB biotech, Ortenberg, Germany) with a standard curve showing good linearity in the range 2.5–150 µg/mL peptide (R^2 = 0.997).

2.6. Proteolysis and bactericidal effect after proteolysis

Proteolytic protection was investigated after incubation of the cubosome dispersions with *Pseudomonas aeruginosa* elastase (PE) (261.0 units/mg, BioCol GmbH, Potsdam, Germany) or human neutrophil elastase (HNE) (20.0 units/mg, Calbiochem, La Jolla, USA) as previously described [20]. The peptide degradation was visualized by gel electrophoresis using Coomassie Brilliant Blue staining. Band intensities were quantified by Molecular Imager Gel DOC with Image Lab Software (BioRad, Hercules, USA). Radial diffusion assay was performed on the formulations before and after incubation with elastases, using *Escherichia coli* (ATCC 25922) and *Staphylococcus aureus* (ATCC 25923) to evaluate the bactericidal properties after proteolysis. Each experiment was repeated 4 times.

2.7. In vitro skin irritation

The skin irritating potential of LL-37 loaded cubosomes was investigated by irritation testing according to OECD TG 439 [46] using the In Vitro EpiDerm™ Skin Irritation Test (EPI-200-SIT, MatTek In Vitro Life Science Laboratories, Bratislava, Slovakia). The test consists of exposing the material to a reconstructed human epidermis model, followed by a cell viability assay using yellow water-soluble 3-(4,5-dimethylthiazol-2-yl)-2,5-diphenyltetrazoliumbromid (MTT; Sigma-Aldrich, St. Louis, MO), which is metabolically reduced to a blue-violet insoluble formazan in viable cells. The material to be tested, positive (5% sodium dodecyl sulfate (SDS)) and negative control (Dulbecco's phosphate-buffered saline (DPBS) without Ca^{2+} and Mg^{2+} were added to the skin models for 60 min, thoroughly washed with DPBS and allowed to recover in assay medium for 42 h in the incubator. Then, MTT solution was added to the skin models and incubated for an additional 3 h at 37 ± 1 °C in 5 ± 1% CO_2. MTT solution was removed, 2-propanol added and the plates were shaken rapidly for two hours. The solution from the individual skin models were homogenized and transferred to a 96 well plate for absorbance measurement at 570 nm followed by calculation of the viability of the keratinocyte cells, relative to the negative control. Skin irritation potential of the sample is expected if the remaining relative cell viability is below 50%.

2.8. Ex vivo pig skin wound infection model

The bactericidal effect of LL-37 loaded cubosomes was investigated using an *ex vivo* pig skin wound infection model [11,47–49]. Briefly, the bacteria (*Staphylococcus aureus,* ATCC 29213) were grown overnight and diluted to a final density of 1×10^7 colony forming units (CFU)/mL in brain heart infusion broth diluted 100 times in sterile H_2O (BHI-100). Punch biopsies were made in the shaved and cleaned pig skin, approximately 0.5–1 mm deep and 3 mm in diameter. Each biopsy was infected by addition of 100 µL of the bacteria suspension and incubated for two hours at 37 °C. 100 µL of the cubosome samples, pure LL-37 or BHI-100 (negative control) were added to each wound and incubated for 4 h at 37 °C. The bacteria were harvested by adding 500 µL of Kligman buffer followed by rubbing the wound area gently with an inoculating loop. The suspension was transferred to a 5 mL tube with 1 mL 2X diluted Kligman buffer, the procedure was repeated once and the two fractions of bacteria suspension from the infected area were pooled. The bacteria suspensions were serial diluted and seeded on horse blood agar plates. The plates were incubated at 37 °C overnight followed by counting the colonies. Each sample was tested on five infected wounds.

3. Results

3.1. Characterization of the cubosomes

Particle size and size distributions are presented in Fig. 1. Differences in particle size and their distributions were observed among the

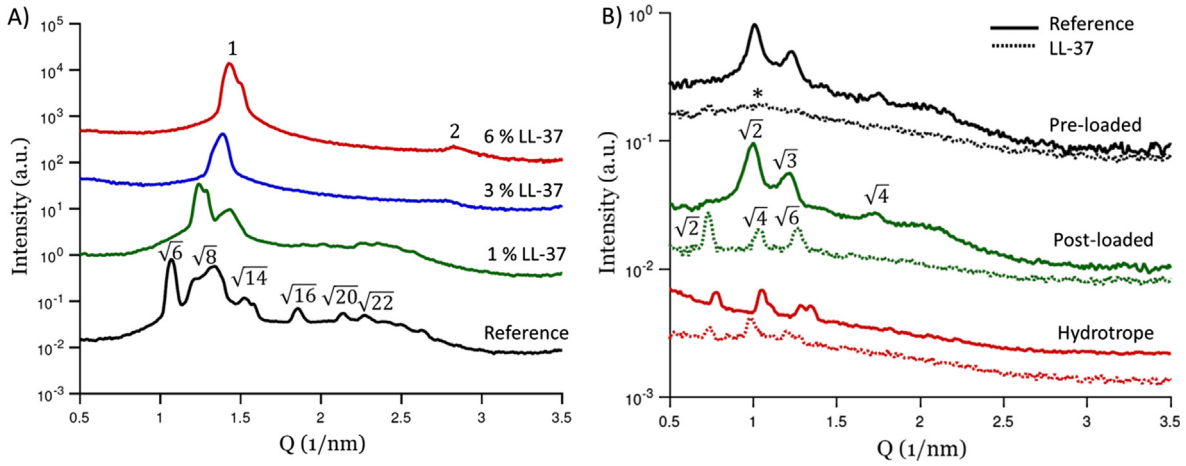

Fig. 2. SAXS diffractograms of LC gels, used for preparation of pre-loaded LCNPs (A) and of cubosome dispersions containing 1.5 mg/mL LL-37 (dashed lines) (B). References contain no LL-37. Peak spacing ratios for cubic Ia3d (Reference, A), lamellar (6% LL-37, A), cubic Pn3m (Post-loaded reference, B) and Im3m (Post-loaded with LL-37) are indicated in the figures.

preparation techniques. Pre-loaded particles had a particle size around 130 nm with a narrow size distribution (PDI ~0.15). The heat-treatment of the cubosomes used for post-loading was found to increase the particle size. Cubosomes prepared via the hydrotrope method displayed a fairly small particle size, taken into account the very gentle shearing applied (magnetic stirring). However, a broad particle size distribution was observed. Interestingly, the presence of LL-37 decreased the mean particle size for all prepared formulations, compared to references without peptide.

The liquid crystalline structure of the gels pre-loaded with LL-37 and of cubosomes prepared by the different techniques were investigated by SAXS, see Fig. 2A and B, respectively. It was found that an increased concentration of LL-37 in the LC gel induced a transition from cubic Ia3d to lamellar phase. As a consequence, the corresponding dispersion of the LC gel showed a broad peak at $q = 1.05\ nm^{-1}$ (marked with * in Fig. 2A), most likely due to presence of vesicles. Traces of cubic Im3m were also detected, indicating a presence of small fraction cubosomes. A reduction in lattice parameter of the cubic Ia3d cubic LC gel was observed at 1% LL-37 incorporation, compared to reference without peptide. Post-loaded cubosomes displayed a change from cubic Pn3m to Im3m after addition of LL-37. Particles prepared via the hydrotrope method displayed presence of both cubic Pn3m and Im3m structure. Calculated lattice parameters for the detected LC structures are presented in Table 1.

Release of LL-37 from the cubosomes was quantified trough dialysis and a fluorescamine assay. Data showed that LL-37 is strongly associated to the particles, as almost no release of peptide was detected during the 24 h dialysis, see Fig. 3. Only small release of LL-37 from hydrotrope cubosomes was observed (< 2%). Pure LL-37 solution (no cubosomes) at the same concentrations as in the cubosomes did cross the dialysis membrane Figs. 1 and 3D).

3.2. In vitro and ex vivo studies

Results from the skin irritation test, proteolysis, and bacterial killing after proteolysis studies, are shown in Fig. 4. The viability of the keratinocyte cells in the epidermis model was found not to be negatively affected by the exposure of cubosomes, indicating no skin irritation (Fig. 4A). No significant difference was observed for any type of cubosomes, with or without LL-37. The positive (5% SDS) and negative (DPBS) controls performed as expected. Pure LL-37 was found to be almost completely degraded after exposure to the elastases and the proteolysis test showed that cubosomes protected LL-37 from degradation by HNE and PE (Fig. 4B). It was also shown that LL-37 remained intact in the cubosomes prior to enzyme exposure. After the proteolysis, the bacterial killing properties against *Escherichia coli* and *Staphylococcus aureus* were examined using RDA (Fig. 4C and D). A trend was observed that the LL-37 loaded cubosomes showed a bactericidal effect after proteolysis, compared to pure LL-37 that had lost all its antimicrobial activity. However, the bactericidal effect of the particles with LL-37 was reduced compared to LL-37 not exposed to enzyme. Post-loaded and hydrotrope cubosomes did not display any activity against *Staphylococcus aureus*.

Results from the *ex vivo* pig skin wound infection model is presented in Fig. 5. All cubosomes displayed a reduced bactericidal effect compared to pure LL-37 at same concentrations. Cubosomes without LL-37 surprisingly displayed a bacterial killing effect. Pre-loaded cubosomes appeared to be most efficient at 0.5 mg/mL peptide loading, while

Table 1
Lattice parameters of LC gels used to prepare pre-loaded cubosomes and of cubosome dispersions containing 1.5 mg/mL LL-37 prepared by pre-loading, post-loading and the hydrotrope method.

Manufacturing method	Type	LL-37 concentration (gels w%, dispersions mg/mL)	Ia3d (Å)	Pn3m (Å)	Im3m (Å)	Lamellar (Å)
Pre	gel	0	144.2			
Pre	gel	1	124.9			
Pre	gel	3				45.3
Pre	gel	6				44.6
Pre	LCNPs	0		88.5		
Pre	LCNPs	1.5			119.4[a]	58.3
Post	LCNPs	0		89.0		
Post	LCNPs	1.5			121.5	
Hydrotrope	LCNPs	0		84.5	113.7	
Hydrotrope	LCNPs	1.5			124.1	

[a] Traces.

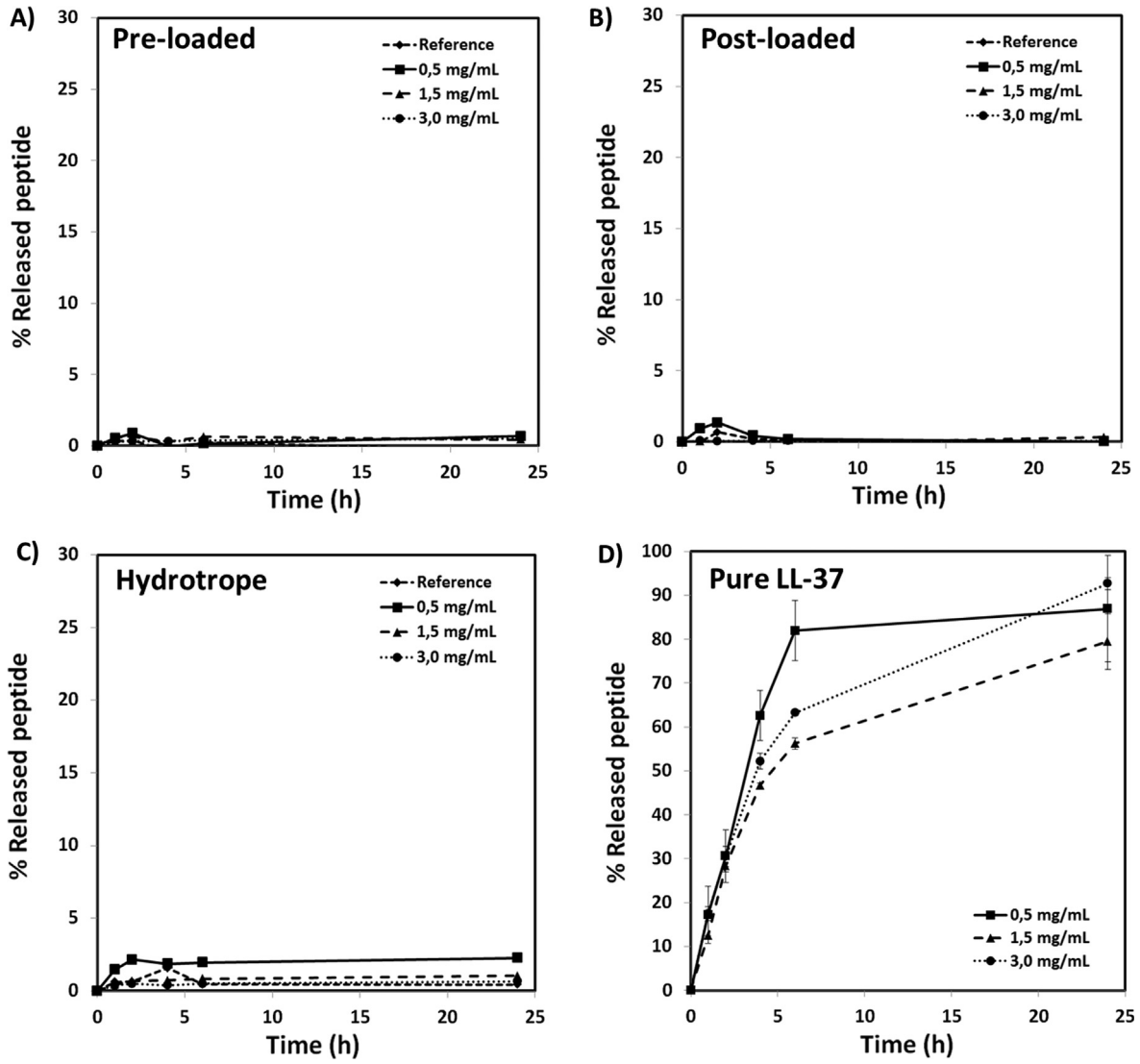

Fig. 3. Release of LL-37 from cubosomes prepared by (A) pre-loading, (B) post-loading, (C) hydrotrope and (D) pure LL-37 solution without cubosomes. Data is presented as mean ± standard deviation (N = 2).

hydrotrope particles performed modest. Pure LL-37 displayed a strong bacterial killing and killed > 95% of the bacteria over the 4 h application period, with a dose–response dependency.

4. Discussion

Particle size and size distributions of the cubosome dispersions differed between the preparation protocols, in line with previous observations [19–21,42,44]. The size of the cubosomes decreased when LL-37 was included. This change in size might be a result of LL-37's membrane disruptive properties and ability to interact with lipid membranes [50,51], enabling easier fragmentation of the particles. Sonication of bulk LC gels (pre-loading) resulted in dispersions with smallest particles and narrowest particle size distribution. Cubosomes prepared via the hydrotrope method resulted in relatively small particles considering the very low shearing forces applied during the preparation (magnetic stirring). Interestingly, the post-loaded particles decreased in size upon increased LL-37 loading, while the size distribution (PDI) of particles increased. This indicates that LL-37 has a strong influence on the pre-formed cubosomes, especially at the two highest concentrations 1.5 and 3 mg/mL. Cubosomes are often surrounded by vesicular structures at the particle-water interface [52] and the high LL-37 concentration may affect/solubilize these structures. However, at lower particle to peptide ratio, LL-37 was previously shown not to have any significant influence on GMO-based cubosomes as visualized by cryo-TEM imaging [19,20].

Particles in the size range 400–700 nm are advantageous to use in dermal applications since they reach deeper into the skin trough the hair follicles [53,54]. Hence, the post-loaded cubosomes are suitable for follicular delivery. However, the hair follicles might be damaged or non-present in damaged or infected skin making this rout less accessible. From a practical perspective, the hydrotrope preparation methodology is very interesting since it does not involve high shearing forces that may induce local heating or high energy consuming steps.

As the LL-37 concentration was increased in the pre-loaded dispersions, the LC structure changed from cubic Pn3m to contain vesicles and traces of cubic Im3m phase. This was in line with recent findings showing that cubosomes are prone to phase change to sponge-like particles and vesicles at high LL-37 loadings, giving rise to a broad diffraction peak in SAXS [23]. Interestingly, the peptide loading strategy influenced the structure of the cubosomes. The pre-loaded particles did mainly consist of vesicles, according to SAXS-data, while post-loaded and hydrotrope cubosomes did display presence of cubic Im3m phase. The differences in structure may be due to variations of LL-37 concentration in the interior of the cubosomes. In case of pre-loading, LL-37 is assumed to be almost completely encapsulated and

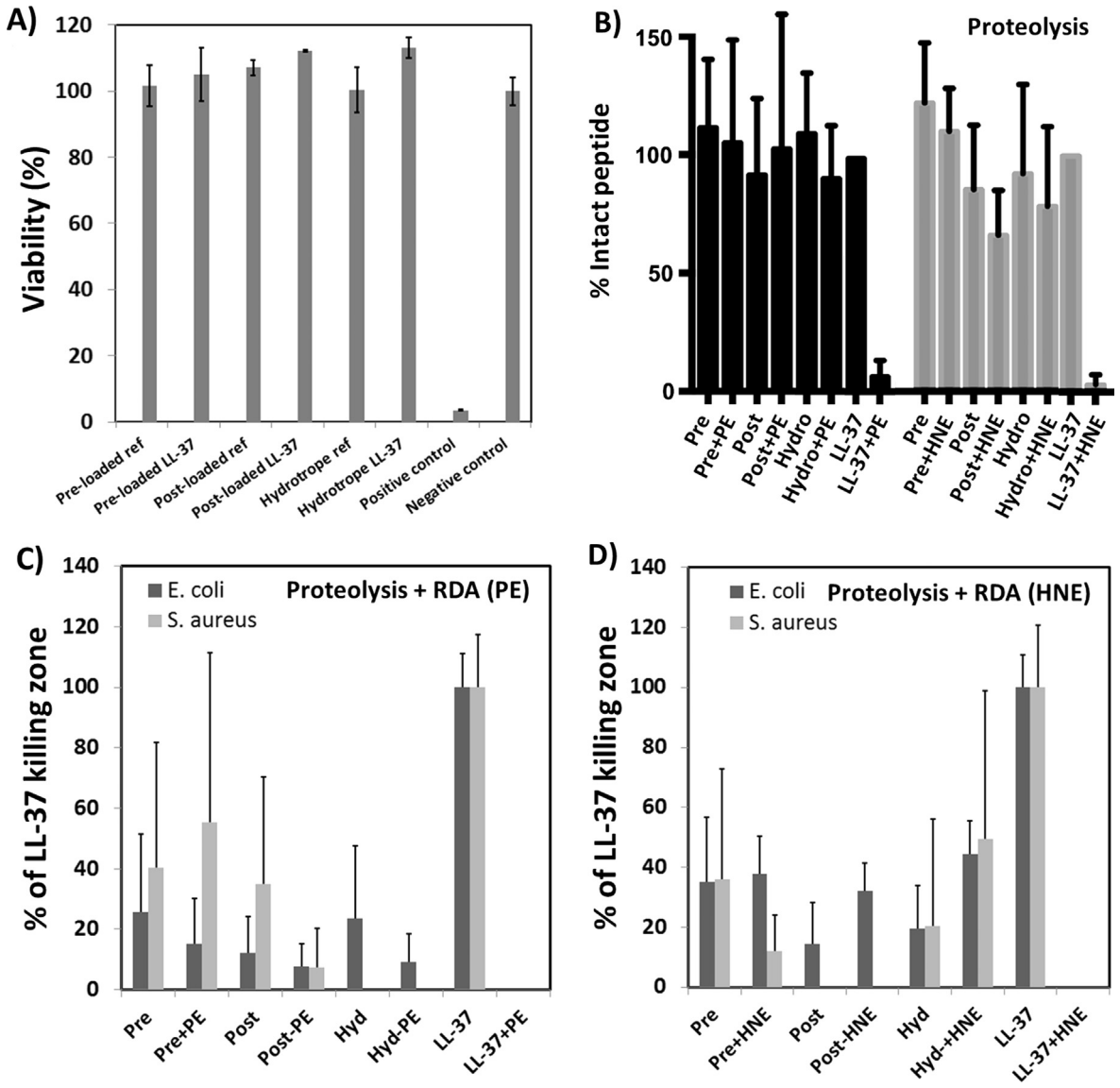

Fig. 4. Skin irritation potential as viability of keratinocyte cells after exposure to cubosomes with and without LL-37 (A), proteolytic protection of LL-37 loaded cubosomes (B), antimicrobial effect after proteolysis with PE (C) and HNE (D) followed by RDA presented as % of pure LL-37 killing zone (no enzyme). Data is reported as mean ± standard deviation (n = 3 in A, n = 5 for PE and n = 3 for HNE in B and n = 4 in C and D).

evenly distributed through the particles, while LL-37 is mainly associated to the surface during post-loading of cubosomes [20]. Thus, one would not expect that surface-associated LL-37 to change the LC structure of the whole cubosome. Localization of LL-37 at the surface of pre- and post-loaded cubosomes was indicated previously by zeta-potential measurements [19,20]. Data showed that the zeta-potential increased from negative (about −15 mV) to positive (+3 to +11 mV) as a consequence of LL-37 addition to the particles. For pre-loaded and hydrotrope prepared cubosomes a complete encapsulation of LL-37 inside the particles is unlikely. The fraction not encapsulated in the interior of the nanoparticles is likely to adsorb to the negative surface of the cubosomes, as for the cubosomes post-loaded with LL-37. The release studies showed no release of LL-37 from the cubosomes during the 24 h incubation, indicating a strong association of the peptide to the particles. These findings are further supported by the proteolysis studies, which showed protection of LL-37 from enzymatic degradation, suggesting that the elastases cannot access the peptide whilst associated to the cubosomes. The findings are in line with previous work [20] and with studies showing that membrane bound LL-37 is less susceptible to undergo proteolysis [55]. If a large fraction of peptide is not encapsulated, one would expect to observe partial degradation of the peptide in the formulation, which was not the case.

The skin irritation test suggested that the cubosomes had no skin irritating potential, making them suitable for topical applications. The model contains human-derived epidermal keratinocytes, cultured to form a multilayered highly differentiated model of the human epidermis. It consists of organized basal, spinous and granular layers, and a multilayered stratum corneum containing intercellular lamellar lipid layers arranged in patterns analogous to those found *in vivo*. Hence, the model is very sophisticated and mimics *in vivo* conditions well. Due to the fact that the particles prepared via the different methodologies have an almost identical composition, no major differences were expected, which was also the case. Hemolytic and cytotoxic properties of GMO-based cubosomes have been reported [56,57], which may restrict the rout of administration to topical. It has also been shown that cubosomes interact with plasma components resulting in destabilization of the particles [58].

The *ex vivo* wound infection model showed that the LL-37 in buffer solution was more efficient in killing *Staphylococcus aureus* than any of the LL-37 loaded cubosomes. This observation may be explained by the

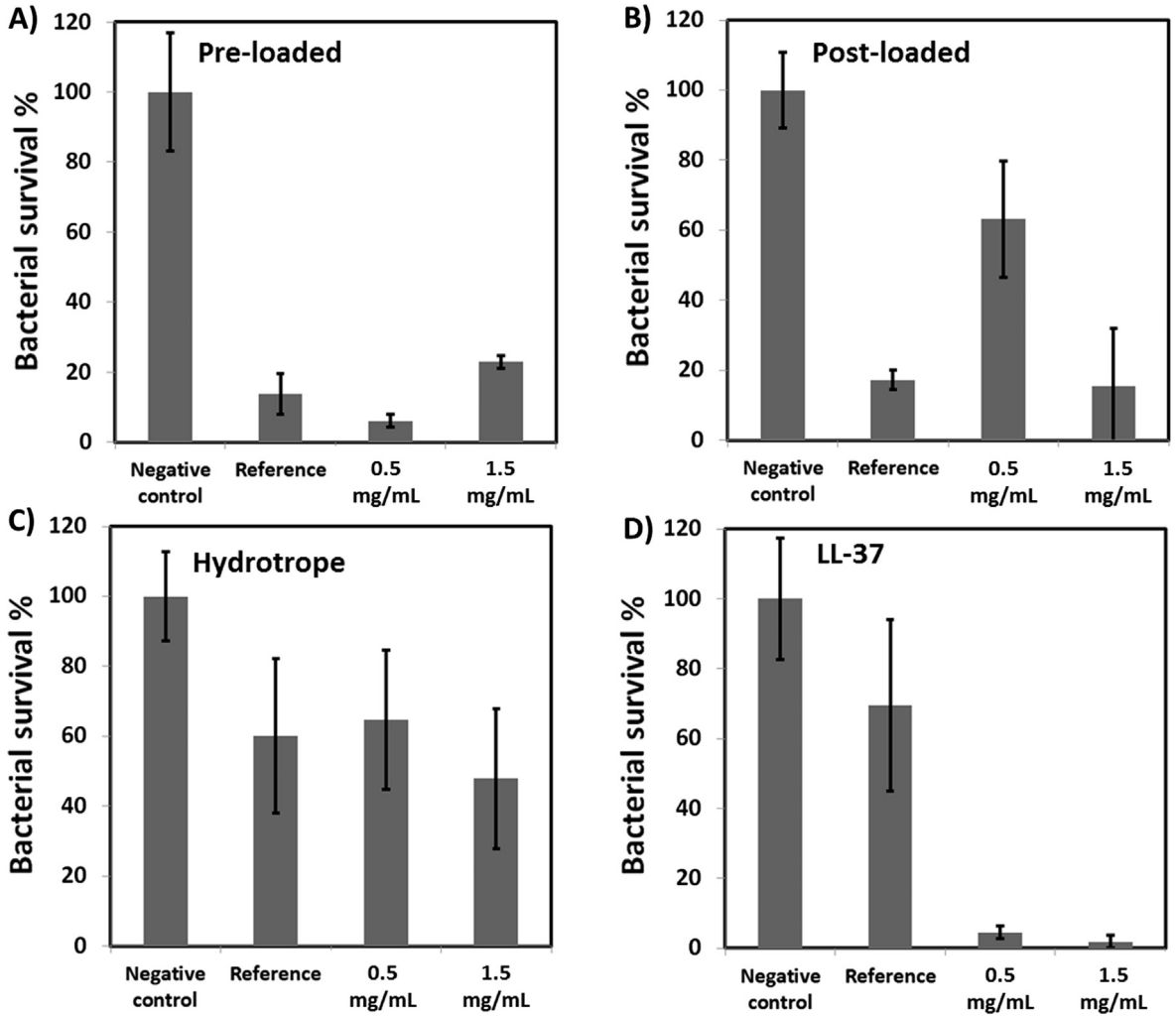

Fig. 5. Ex-vivo pig skin wound infection model. Survival of *Staphylococcus aureus* presented as % of negative control (approximately 10^7 CFU/mL). "Reference" refers to cubosome without LL-37 in panel A-C, whilst in D it refers to sodium acetate buffer. Negative control is 100X diluted BHI in MilliQ-water. Data is presented as mean ± standard error of mean (N = 5).

fact that the amount of available "free" peptide is reduced due to encapsulation in the cubosomes. Hence, if only the non-encapsulated peptide is giving rise to bacterial killing, a reduction in activity would be expected. Previously we showed that AMPs encapsulated in cubosomes sometimes can reduce the antimicrobial effect (minimum inhibitory concentration tests and time kill experiments, planktonic bacteria), compared to pure peptide [19]. However, the delivery mechanism and antibacterial properties of LL-37 loaded cubosomes may differ among planktonic bacteria and bacteria in this *ex vivo* model. It was shown that if AMPs are too well encapsulated, e.g. in hexosomes, the antibacterial efficiently can be reduced. Our data indicate that pre-loaded cubosomes kill bacteria slightly better, compared to the cubosomes prepared by the two other methodologies. The small particle size and narrow size distribution (~130 nm, PDI 0.15) creates a great surface area that seems to be beneficial for delivery of LL-37. It might facilitate for many interaction points between the particles and bacteria. Surprisingly, the pre-loaded cubosomes killed bacteria more efficient at 0.5 mg/mL LL-37 compared to 1.5 mg/mL. Previous investigations showed that pre-loaded cubosomes at 0.5 mg/ mL LL-37 had a cubic Im3m structure [19]. Cryo-TEM investigations of the particles displayed a large fraction of vesicles as well as cubosome particles with internal structure. However, at the highest LL-37 loading investigated herein, SAXS-data indicated mainly presence of less structured particles, such as vesicles. Hence, our data may indicate a slightly better antibacterial effect of dispersions containing a larger fraction of cubosomes.

Penetration of nanoparticles in biofilms is mainly limited by diffusion and interaction with the biofilm matrix constituents [59]. Hence, the small pre-loaded particles are beneficial from a diffusion perspective. However, the proteolytic protection offered by the cubosomes, resulting in an increased bacterial killing after exposure to enzymes, does favor the use of particles. Efficient proteolytic protection will facilitate for translation of proteolytic sensitive AMPs to the clinic.

Surprisingly, cubosomes without any LL-37 did also display an antimicrobial effect, something not observed in minimum inhibitory (MIC) tests using planktonic bacteria [19,20,23]. However, the concentration of particles was much lower in the MIC tests which may explain the difference in activity. In the *ex vivo* model the cubosome dispersions are used as is, without further dilution, which is not the case for MIC-tests. Hence, a cubosome concentration of 5% might be suffocating for the bacteria and suppresses the growth.

5. Conclusions

In this study we have further elaborated on the use of cubosomes for topical delivery of LL-37. We confirmed that high LL-37 loadings in the cubosomes induced formation of lamellar phase and in turn vesicles upon dispersion into particles. No release of LL-37 was observed from

the cubosomes resulting in a superior protection of LL-37 against enzyme attacks. Hence, a significant better bactericidal effect was observed for cubosomes with encapsulated LL-37 after enzyme exposure, compared to pure LL-37 that had lost its bactericidal effect after proteolysis. Moreover, cubosomes with and without LL-37 did not induce skin irritation, thus being suitable for topical application. Hence, a good encapsulation of LL-37 in the cubosomes is a necessity to achieve good proteolytic protection of LL-37, but the encapsulations serve as disadvantage in terms of the antibacterial properties. Cubosomes designed for trigged release of peptide to increase the local concentration of free peptide might overcome the reduction of antibacterial effect as observed in this study.

Acknowledgements

The research performed in this study was funded by the European Union's Seventh Framework Program (FP7/2007-2013), under Grant Agreement No. 604182 within the FORMAMP project.

References

[1] WHO, Antimicrobial resistance: global report on surveillance, 2014.
[2] L. Czaplewski, et al., Review: alternatives to antibiotics—a pipeline portfolio review, Lancet. Infect. Dis. 16 (2016) 239–251.
[3] G.J. Moet, et al., Contemporary causes of skin and soft tissue infections in North America, Latin America, and Europe: Report from the SENTRY Antimicrobial Surveillance Program (1998–2004), Diagn. Microbiol. Infect. Dis. 57 (1) (2007) 7–13.
[4] D. Church, et al., Burn wound infections, Clin. Microbiol. Rev. 19 (2) (2006) 403–434.
[5] A. Giacometti, et al., Epidemiology and microbiology of surgical wound infections, J. Clin. Microbiol. 38 (2) (2000) 918–922.
[6] F.D. Lowy, Antimicrobial resistance: the example of Staphylococcus aureus, J. Clin. Invest. 111 (9) (2003) 1265–1273.
[7] D.J. Leaper, et al., Surgical site infection - a European perspective of incidence and economic burden, Int. Wound J. 1 (4) (2004) 247–273.
[8] M.S. Dryden, Complicated skin and soft tissue infection, J. Antimicrob. Chemother. 65 (suppl_3) (2010) iii35–iii44.
[9] M. Pasupuleti, A. Schmidtchen, M. Malmsten, Antimicrobial peptides: key components of the innate immune system, Crit. Rev. Biotechnol. 32 (2) (2012) 143–171.
[10] R.E.W. Hancock, H.-G. Sahl, Antimicrobial and host-defense peptides as new anti-infective therapeutic strategies, Nat. Biotechnol. 24 (12) (2006) 1551–1557.
[11] A. Schmidtchen, et al., Boosting antimicrobial peptides by hydrophobic oligopeptide end tags, J. Biol. Chem. 284 (26) (2009) 17584–17594.
[12] R. Eckert, Road to clinical efficacy: challenges and novel strategies for antimicrobial peptide development, Future Microbiol. 6 (6) (2011) 635–651.
[13] M. Mahlapuu, et al., Antimicrobial peptides: an emerging category of therapeutic agents, Frontiers Cell. Infect. Microbiol. 6 (2016).
[14] R. Nordström, M. Malmsten, Delivery systems for antimicrobial peptides, Adv. Colloid Interface Sci. 242 (2017) 17–34.
[15] A. Angelova, et al., Self-assembled multicompartment liquid crystalline lipid carriers for protein, peptide, and nucleic acid drug delivery, Acc. Chem. Res. 44 (2) (2010) 147–156.
[16] A. Angelova, et al., Advances in structural design of lipid-based nanoparticle carriers for delivery of macromolecular drugs, phytochemicals and anti-tumor agents, Adv. Colloid Interface Sci. 249 (2017) 331–345.
[17] N. Matougui, et al., Lipid-based nanoformulations for peptide delivery, Int. J. Pharm. 502 (1–2) (2016) 80–97.
[18] X. Mulet, B.J. Boyd, C.J. Drummond, Advances in drug delivery and medical imaging using colloidal lyotropic liquid crystalline dispersions, J. Colloid Interface Sci. 393 (2013) 1–20.
[19] L. Boge, et al., Lipid-based liquid crystals as carriers for antimicrobial peptides: phase behavior and antimicrobial effect, Langmuir 32 (17) (2016) 4217–4228.
[20] L. Boge, et al., Cubosomes post-loaded with antimicrobial peptides: characterization, bactericidal effect and proteolytic stability, Int. J. Pharm. 526 (1–2) (2017) 400–412.
[21] L. Boge, et al., Freeze-dried and re-hydrated liquid crystalline nanoparticles stabilized with disaccharides for drug-delivery of the plectasin derivative AP114 antimicrobial peptide, J. Colloid Interface Sci. 522 (2018) 126–135.
[22] T.G. Meikle, et al., Incorporation of antimicrobial peptides in nanostructured lipid membrane mimetic bilayer cubosomes, Colloids Surf., B 152 (2017) 143–151.
[23] M. Gontsarik, et al., Antimicrobial peptide-driven colloidal transformations in liquid-crystalline nanocarriers, J. Phys. Chem. Lett. 7 (17) (2016) 3482–3486.
[24] L.D. Lozeau, M.W. Rolle, T.A. Camesano, A QCM-D study of the concentration- and time-dependent interactions of human LL37 with model mammalian lipid bilayers, Colloids Surf., B. 167 (2018) 229–238.
[25] R. Ramos, et al., Wound healing activity of the human antimicrobial peptide LL37, Peptides 32 (7) (2011) 1469–1476.
[26] A.A. Strömstedt, et al., Evaluation of strategies for improving proteolytic resistance of antimicrobial peptides by Using Variants of EFK17, an Internal Segment of LL-37, Antimicrob. Agents Chemother. 53 (2) (2009) 593–602.
[27] A. Gronberg, et al., Treatment with LL-37 is safe and effective in enhancing healing of hard-to-heal venous leg ulcers: a randomized, placebo-controlled clinical trial, Wound Repair Regen 22 (5) (2014) 613–621.
[28] M. Shahmiri, et al., Membrane core-specific antimicrobial action of cathelicidin LL-37 peptide switches between pore and nanofibre formation, Sci. Rep. 6 (2016) 38184.
[29] R. Sood, et al., Binding of LL-37 to model biomembranes: insight into target vs host cell recognition, Biochim. Biophys. Acta (BBA) – Biomembr. 1778 (4) (2008) 983–996.
[30] D. Vandamme, et al., A comprehensive summary of LL-37, the factotum human cathelicidin peptide, Cell. Immunol. 280 (1) (2012) 22–35.
[31] S. Jain, et al., Recent advances in lipid-based vesicles and particulate carriers for topical and transdermal application, J. Pharm. Sci. 106 (2) (2017) 423–445.
[32] M. Sala, et al., Lipid nanocarriers as skin drug delivery systems: properties, mechanisms of skin interactions and medical applications, Int. J. Pharm. 535 (1) (2018) 1–17.
[33] Y. Zhai, G. Zhai, Advances in lipid-based colloid systems as drug carrier for topic delivery, J. Control. Release 193 (2014) 90–99.
[34] L. Lopes, et al., Reverse hexagonal phase nanodispersion of monoolein and oleic acid for topical delivery of peptides: in vitro and in vivo skin penetration of cyclosporin A, Pharm. Res. 23 (6) (2006) 1332–1342.
[35] L.B. Lopes, F.F.F. Speretta, M.V.L.B. Bentley, Enhancement of skin penetration of vitamin K using monoolein-based liquid crystalline systems, Eur. J. Pharm. Sci. 32 (3) (2007) 209–215.
[36] T. Rattanapak, et al., Comparative study of liposomes, transfersomes, ethosomes and cubosomes for transcutaneous immunisation: characterisation and in vitro skin penetration, J. Pharm. Pharmacol. 64 (11) (2012) 1560–1569.
[37] E. Esposito, et al., Cubosome dispersions as delivery systems for percutaneous administration of indomethacin, Pharm. Res. 22 (12) (2005) 2163–2173.
[38] S.R. Seo, et al., In vivo hair growth-promoting efficacies of herbal extracts and their cubosomal suspensions, J. Ind. Eng. Chem. 19 (4) (2013) 1331–1339.
[39] U. Bazylińska, et al., Polymer-free cubosomes for simultaneous bioimaging and photodynamic action of photosensitizers in melanoma skin cancer cells, J. Colloid Interface Sci. 522 (2018) 163–173.
[40] C.V. Kulkarni, et al., Monoolein: a magic lipid? Phys. Chem. Chem. Phys.: PCCP 13 (8) (2011) 3004.
[41] U.S. Food and Drug Administration (FDA), Inactive Ingredient Search for Approved Drug Products, [cited 2018 2018-10-11]; (Available from: < https://www.accessdata.fda.gov/scripts/cder/iig/index.cfm >).
[42] J. Barauskas, et al., Cubic phase nanoparticles (cubosome): principles for controlling size, structure, and stability, Langmuir 21 (6) (2005) 2569–2577.
[43] P. Spicer, Cubosome processing: industrial nanoparticle technology development, Chem. Eng. Res. Des. 83 (11) (2005) 1283–1286.
[44] P.T. Spicer, et al., Novel process for producing cubic liquid crystalline nanoparticles (cubosomes), Langmuir 17 (19) (2001) 5748–5756.
[45] S.T. Hyde, Identification of Lyotropic Liquid crystalline Mesophases, in: K. Holmberg (Ed.), Handbook of Applied Surface and Colloid Chemistry, John Wiley & Sons, Ltd., 2001, pp. 299–332.
[46] OECD, Test No. 439: In Vitro Skin Irritation - Reconstructed Human Epidermis Test Method, OECD Publishing, 2013.
[47] C. Björn, et al., Anti-infectious and anti-inflammatory effects of peptide fragments sequentially derived from the antimicrobial peptide centrocin 1 isolated from the green sea urchin Strongylocentrotus droebachiensis, AMB Express 2 (2012) 67–167.
[48] C. Bjorn, et al., Anti-infective efficacy of the lactoferrin-derived antimicrobial peptide HLR1r, Peptides 81 (2016) 21–28.
[49] E. Myhrman, et al., The novel antimicrobial peptide PXL150 in the local treatment of skin and soft tissue infections, Appl. Microbiol. Biotechnol. 97 (7) (2013) 3085–3096.
[50] D. Xhindoli, et al., The human cathelicidin LL-37–A pore-forming antibacterial peptide and host-cell modulator, Biochim. Biophys. Acta 1858 (3) (2016) 546–566.
[51] X. Zhang, et al., Dual functions of the human antimicrobial peptide LL-37-target membrane perturbation and host cell cargo delivery, Biochim. Biophys. Acta 1798 (12) (2010) 2201–2208.
[52] D. Demurtas, et al., Direct visualization of dispersed lipid bicontinuous cubic phases by cryo-electron tomography, Nat. Commun. 6 (2015) 8915.
[53] A.R.M. Coates, G. Halls, Y. Hu, Novel classes of antibiotics or more of the same? Br. J. Pharmacol. 163 (1) (2011) 184–194.
[54] A. Patzelt, et al., Selective follicular targeting by modification of the particle sizes, J. Control. Release 150 (1) (2011) 45–48.
[55] Z. Oren, et al., Structure and organization of the human antimicrobial peptide LL-37 in phospholipid membranes: relevance to the molecular basis for its non-cell-selective activity, Biochem. J. 341 (Pt 3) (1999) 501–513.
[56] J. Barauskas, et al., Interactions of lipid-based liquid crystalline nanoparticles with model and cell membranes, Int. J. Pharm. 391 (1–2) (2010) 284–291.
[57] S. Milak, A. Zimmer, Glycerol monooleate liquid crystalline phases used in drug delivery systems, Int. J. Pharm. 478 (2) (2015) 569–587.
[58] W. Leesajakul, et al., Interaction of cubosomes with plasma components resulting in the destabilization of cubosomes in plasma, Colloids Surf., B 34 (4) (2004) 253–258.
[59] A. Gupta, R.F. Landis, V.M. Rotello, Nanoparticle-based antimicrobials: surface functionality is critical, F1000 Res. 5 (2016) F1000 (Faculty Rev-364).